Synthesis and Discovery of Macrocyclic Polyoxygenated Bis-7-azaindolylmaleimides as a Novel Series of Potent and Highly Selective Glycogen Synthase Kinase-3β Inhibitors

Gee-Hong Kuo,* Catherine Prouty, Alan DeAngelis, Lan Shen, David J. O'Neill, Chandra Shah, Peter J. Connolly, William V. Murray, Bruce R. Conway, Peter Cheung, Lori Westover, Jun Z. Xu, Richard A. Look, Keith T. Demarest, Stuart Emanuel, Steven A. Middleton, Linda Jolliffe, Mary Pat Beavers, and Xin Chen

Drug Discovery Division, Johnson and Johnson Pharmaceutical Research and Development, L.L.C., 1000 Route 202, P.O. Box 300, Raritan, New Jersey 08869

Received March 11, 2003

Attempts to design the macrocyclic maleimides as selective protein kinase C γ inhibitors led to the unexpected discovery of a novel series of potent and highly selective glycogen synthase kinase-3β (GSK-3β) inhibitors. Palladium-catalyzed cross-coupling reactions were used to synthesize the key intermediates **17** and **22** that resulted in the synthesis of novel macrocycles. All three macrocyclic series (bisindolyl-, mixed 7-azaindoleindolyl-, and bis-7-azaindolylmaleimides) were found to have submicromolar inhibitory potency at GSK-3β with various degrees of selectivity toward other protein kinases. To gain the inhibitory potency at GSK-3β, the ring sizes of these macrocycles may play a major role. To achieve the selectivity at GSK-3β, the additional nitrogen atoms in the indole rings may contribute to a significant degree. Overall, the bis-7-azaindolylmaleimides **28** and **29** exhibited little or no inhibitions to a panel of 50 protein kinases. Compound **29** almost behaved as a GSK-3β specific inhibitor. Both **28** and **29** displayed good potency in GS cell-based assay. Molecular docking studies were conducted in an attempt to rationalize the GSK-3β selectivity of azaindolylmaleimides.

Introduction

Glycogen synthase kinase-3 (GSK-3) is a serine/threonine protein kinase that was first identified over 20 years ago because of its ability to phosphorylate and inhibit glycogen synthase (GS),[1] the rate-limiting enzyme of glycogen biosynthesis.[2] Mammalian GSK-3 exists as two isoforms, GSK-3α and GSK-3β, sharing 98% homology in their catalytic domain.[3] Both isoforms are ubiquitously expressed in cells and tissues and have similar biochemical properties.[3] Today, it is known that GSK-3 is involved in diverse cellular processes and might have multiple substrates.[4,5] For example, GSK-3 phosphorylates and inhibits the functioning of insulin receptor substrate-1 (IRS-1) and GS, the two key targets in the insulin signaling pathway.[6] Suppression of these targets may limit most insulin-mediated biological responses. In addition, elevated GSK-3 activity was found in diabetic tissues, reinforcing GSK-3 as a promising therapeutic target for insulin resistance and type 2 diabetes. Tau is a known substrate of GSK-3 in vivo. Tau hyperphosphorylation is an early event in neurodegenerative conditions such as Alzheimer's disease and is postulated to promote microtubule disassembly.[7] Inhibition of GSK-3 has also been shown to attenuate apoptotic signals.[8] Therefore, GSK-3 inhibitors may be useful for the treatment of Alzheimer's disease and protection against cell death.[9] Lithium ions and valproic acid have been used as mood stabilizers for the chronic treatment of patients with bipolar disorder. Recently, these compounds have been shown to be GSK-3 inhibitors.[10] Finally, studies on fibroblasts from the GSK-3β knockout mice indicate that inhibition of GSK-3 may be useful in treating inflammatory disorders or diseases through the negative regulation of NFκB activity.[11]

Since Chiron disclosed purines[12] (Scheme 1) are capable of exhibiting GSK-3 inhibitory activities, many chemical series[13,14] (pyrazines, pyrimidines, heterocyclic pyrimidones, aminepyrazoles, bisindolemaleimides, hymenialdisine, paullones, indirubines, and anilinomaleimides) have been developed as ATP competitive GSK-3 inhibitors while thiadiazolidinones[15] were reported to be the first ATP noncompetitive GSK-3 inhibitors. However, except for the anilinomaleimides,[16,17] which were demonstrated as selective GSK-3 inhibitors relative to 24 protein kinases, the majority of the ATP competitive GSK-3 inhibitors all showed significant activities at several other protein kinases. To minimize the potential side effects, it is always desirable to have the clinical agent targeting the enzyme specifically. This article describes the unexpected discovery of macrocyclic polyoxygenated bis-7-azaindolylmaleimides as a novel series of potent and highly selective GSK-3β inhibitors.

Chemistry

The syntheses of macrocyclic bisindolylmaleimides **10**−**13** are shown in Scheme 2. Alkylation of the readily prepared bisindolylmaleimide **1**[18] with the bismesylate **2**−**5**[19] in the presence of Cs_2CO_3 in DMF[20] readily gave the desired cyclic *N*-methylmaleimides **6**−**9**. Conversion of **6**−**9** to the target molecules **10**−**13** were accomplished by hydrolysis and ammonolysis.[20]

The syntheses of mixed 7-azaindoleindolylmaleimides **20** and **21** are shown in Scheme 3. The tributyltin

* To whom correspondence should be addressed. Phone: 908-704-4330. Fax: 908-203-8109. E-mail: gkuo@prdus.jnj.com.

10.1021/jm030115o CCC: $25.00
Published on Web 08/12/2003

Scheme 1

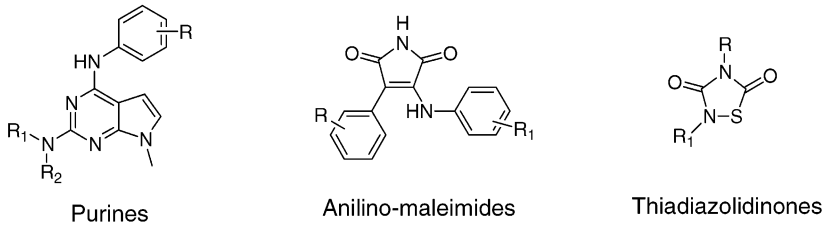

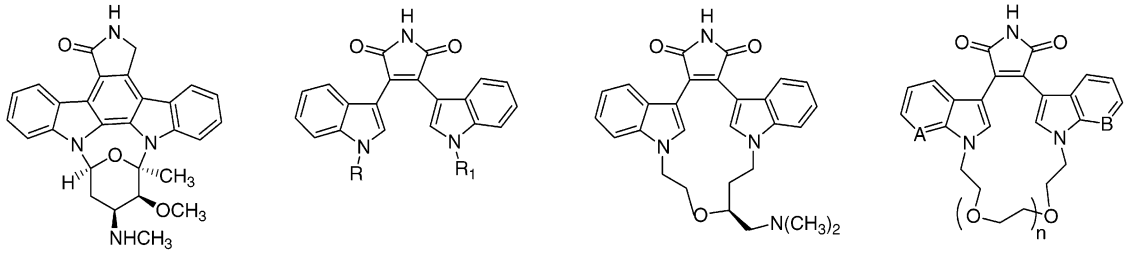

Scheme 2[a]

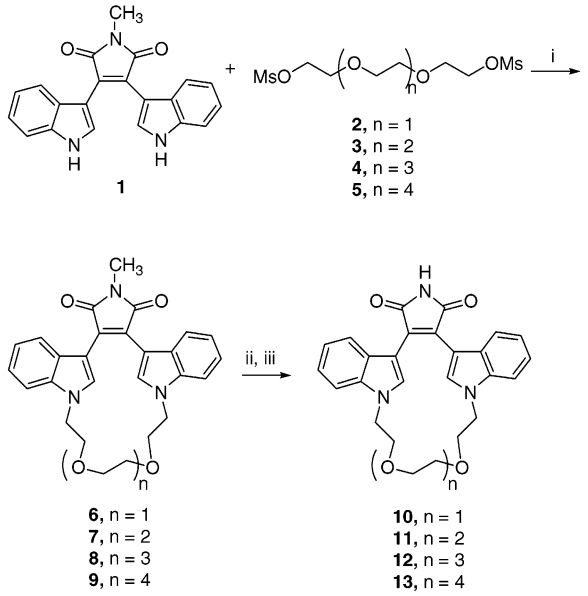

[a] (i) Cs_2CO_3, DMF, 100 °C; (ii) KOH, EtOH, refluxing; (iii) HMDS, DMF, 80 °C.

Scheme 3[a]

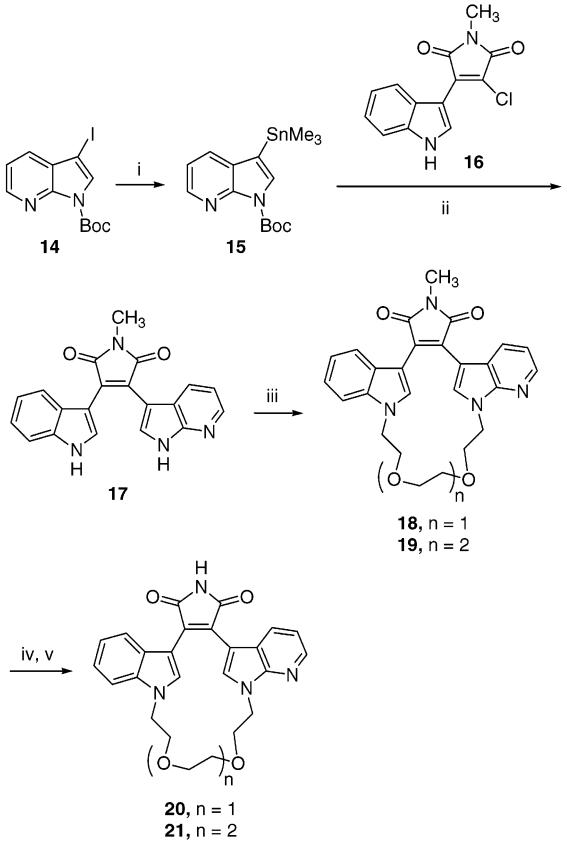

[a] (i) Me_3SnCl, −78 °C, *n*-BuLi; (ii) $PdCl_2(PPh_3)_2$, LiCl, toluene, 95 °C; (iii) **2** and **3**, Cs_2CO_3, DMF, 100 °C; (iv) KOH, EtOH, refluxing; (v) HMDS, DMF, 80 °C.

analogue of **15** was reported to be synthesized from 3-iodo-7-azaindole derivative **14** in 19% yield.[21] It was found that if trimethyltin chloride was mixed with the iodide **14** at −78 °C before the addition of *n*-butyllithium, the yield of **15** was increased to 55−60%. A palladium-catalyzed cross-coupling reaction[22] of **15** with chloroindolylmaleimide **16**[18] gave the deprotected 7-azaindoleindolylmaleimide **17**. To the best of our knowledge, this is the first example of readily available chloromaleimide being used in the palladium catalyzed C−C bond formation reaction.[23] Similar to **1**, alkylation of **17** with the bismesylates **2** and **3** gave cyclic *N*-methylmaleimides **18** and **19**, followed by hydrolysis and ammonolysis to give the target molecules **20** and **21**.

The syntheses of macrocyclic bis-7-azaindolylmaleimides **27**−**30** are shown in Scheme 4. It was demonstrated that condensation of an indole Grignard reagent with 2,3-dichloro-*N*-methylmaleimide in toluene/ether (5:1 ratio by volume) gave bisindolylmaleimide **1** in 93% yield.[18] In contrast, condensation of a 7-azaindole Grignard reagent with 2,3-dichloro-*N*-methylmaleimide in various combinations of toluene, ether, and THF did not generate any detectable amount of bis-7-azaindolylmaleimide **22**.[24] Fortunately, it was found that the palladium-catalyzed cross-coupling reaction of 7-aza-

Scheme 4[a]

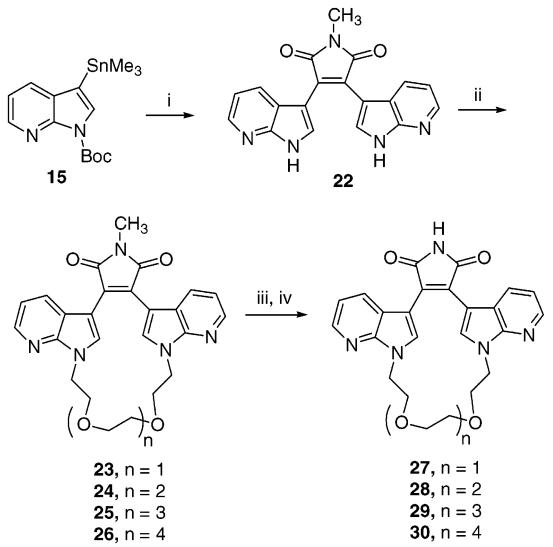

[a] (i) 2,3-Dichloro-*N*-methylmaleimide, $PdCl_2(PPh_3)_2$, LiCl, toluene, 95 °C; (ii) **2**−**5**, Cs_2CO_3, DMF, 100 °C; (iii) KOH, EtOH, refluxing; (iv) HMDS, DMF, 80 °C.

indolestannane **15** with 2,3-dichloro-*N*-methylmaleimide gave the desired coupling product **22**. In analogy to **1**, alkylation of **22** with bismesylates **2**−**5**, followed by hydrolysis and ammonolysis, gave the target molecules **27**−**30**.

Results and Discussion

Lead Discovery. We were originally interested in identifying potent and selective protein kinase C γ (PKCγ) inhibitors for the treatment of chronic pain. However, in a literature search, we could not find any PKCγ selective inhibitors being reported. For example, staurosporine[25] (Scheme 1) was identified as a potent but nonselective PKC inhibitor in 1986 (PKCα, IC_{50} = 0.045 μM; PKCβI, IC_{50} = 0.023 μM; PKCβII, IC_{50} = 0.019 μM; PKCγ, IC_{50} = 0.11 μM).[26] A series of bisindolylmaleimides[27] were shown to have slight selectivity at PKCα over the other PKC isoenzymes. On the other hand, LY333531[26] was the only compound reported that appears to be a potent and selective inhibitor at PKCβII (IC_{50} = 0.006 μM) against PKCα (IC_{50} = 0.36 μM) and PKCγ (IC_{50} = 0.3 μM), despite the high degree of homology that exists among the PKC isoenzymes.[28] Therefore, we decided to synthesize the macrocyclic maleimides target molecules (Scheme 1) to mimic the cyclic structure of LY333531 with the goal of shifting the isoenzyme selectivity from PKCβII to PKCγ.

Four bisindolylmaleimides with polyoxygenated cyclic linkers were first prepared (**10**−**13**, Table 1). All four macrocycles showed micromolar potency at PKCγ (IC_{50} = 1.2−5.17 μM). We next synthesized two challenging macrocycles of mixed 7-azaindoleindolylmaleimides and found that both of them displayed similar potency at PKCγ (IC_{50} = 2.67 μM for **20**; IC_{50} = 1.34 μM for **21**) compared to the corresponding bisindolylmaleimides (IC_{50} = 2.73 μM for **10**; IC_{50} = 1.20 μM for **11**). The addition of one nitrogen atom to one of the indole rings seems to have no impact on the binding affinities of the macrocycles at PKCγ.

We continued our plan to synthesize the bis-7-azaindolylmaleimides. Interestingly, the addition of nitrogen atoms to both of the indole rings dramatically reduced the binding affinities at PKCγ (IC_{50} > 10 μM for **27**−**30**). With disappointment, even the PKCβII selective molecule LY333531 displayed better potency (IC_{50} = 0.3 μM at PKCγ) than all of our macrocycles.

Table 1. Binding Affinities at PKCγ and GSK-3β[a]

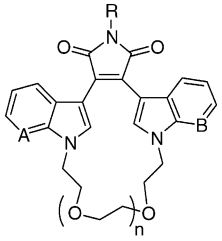

					$IC_{50} \pm SEM$[b] (μM)	
compd	R	A	B	*n*	PKCγ	GSK-3β
10	H	C	C	1	2.73 ± 0.21	0.136 ± 0.019
11	H	C	C	2	1.20 ± 0.12	0.022 ± 0.011
12	H	C	C	3	3.30 ± 0.09	0.026 ± 0.006
13	H	C	C	4	5.17 ± 0.18	0.051 ± 0.007
20	H	C	N	1	2.67 ± 0.19	0.138 ± 0.024
21	H	C	N	2	1.34 ± 0.16	0.017 ± 0.004
27	H	N	N	1	>10	0.620 ± 0.042
28	H	N	N	2	>10	0.034 ± 0.007
29	H	N	N	3	>10	0.048 ± 0.008
30	H	N	N	4	>10	0.403 ± 0.108
7	CH_3	C	C	2	NT[c]	54% inhibition @ 1 μM
18	CH_3	C	N	1	NT[c]	51% inhibition @ 1 μM
LY333531					0.3[d]	NT[c]

[a] Assay details were described in the Experimental Section. [b] SEM: standard error of the mean. [c] Not tested. [d] Reported in ref 26.

To determine whether these molecules show selectivity at PKCγ versus other kinases that we originally designed, we tested the two most potent PKCγ inhibitors (**11** and **21**) against a panel of several kinases. Unexpectedly, both compounds **11** and **21** showed very good potency at GSK-3β (IC_{50} = 22 nM for **11**; IC_{50} = 17 nM for **21**; Table 1). We then tested the remaining molecules at GSK-3β. We observed that both **12** and **13** showed slightly lower potency (IC_{50} = 26 and 51 nM, respectively) while the smallest macrocycles **10** displayed the lowest potency (IC_{50} = 136 nM). Interestingly, the smaller macrocycles **20** in the mixed 7-azaindoleindolylmaleimide series also displayed lower potency (IC_{50} = 138 nM for **20** versus IC_{50} =17 nM for **21**). To our surprise, the bis-7-azaindolylmaleimides **28** and **29** continued to exhibit very good potency at GSK-3β (IC_{50} = 34 nM for **28**; IC_{50} = 48 nM for **29**). Meanwhile, the largest macrocycle **30** showed a lower potency (IC_{50} = 403 nM) and the smallest macrocycle **27** showed the lowest potency (IC_{50} = 620 nM).

There are four points regarding the structure−activity relationships (SAR) that are worthy of note at this stage. First, the optimal ring sizes of the macrocycles to achieve the highest inhibitory potency at GSK-3β in all three series (bisindoles, mixed 7-azaindoleindole, and bis-7-azaindoles) are consistent, namely, 19−22 member rings. Second, the addition of a nitrogen atom to one of the indole rings (**20** or **21**) has no impact on the potency and selectivity at GSK-3β. Third, the addition of nitrogen atoms to both of the indole rings (**27**−**30**) seems to increase the selectivity significantly at GSK-3β without sacrificing too much of the potency. Fourth, the low potency of methylated **7** and **18** (54% inhibition at 1 μM

Table 2. IC_{50} at Selected Kinase Assays[a]

kinase assay	$IC_{50} \pm$ SEM (μM)				
	11	**21**	**28**	**29**	LY333531
GSK-3β	0.022 ± 0.011	0.017 ± 0.004	0.034 ± 0.007	0.048 ± 0.008	
CDK1	1.251 ± 0.031	4.428 ± 0.114	>10	>10	
CDK2	0.992 ± 0.048	2.439 ± 0.395	>10	>10	
VEGF-R	1.450 ± 0.177	3.560 ± 0.401	>10	>10	
PKCα	0.086 ± 0.008	0.673 ± 0.1	>10	>10	0.36[b]
PKCβII	0.006 ± 0.002	0.046 ± 0.006	1.163 ± 0.079	>10	0.006[b]
PKCθ	0.065 ± 0.004	0.835 ± 0.091	>10	>10	
PKA	>10	>10	>10	>10	
calmodulin K	>10	>10	>10	>10	
casein K	>10	>10	>10	>10	

[a] Assay details were described in the Experimental Section. [b] Reported in ref 26.

and 51% inhibition at 1 μM, respectively) suggested that the maleimide NH seems to be critical for the binding.

Kinase Selectivity

Recently, literature reports have described potent cyclin-dependent kinase (CDK) inhibitors that could also inhibit GSK-3β.[29] The acyclic bisindolylmaleimide derivatives were identified as PKC inhibitors[30] and have been reported to be competitive inhibitors of ATP binding presumably by interacting at the ATP binding site.[31] Our compounds **28** and **29**, in common with most of the other protein kinase inhibitors, also inhibited GSK-3β in an ATP competitive manner.[32] We thus evaluated **11**, **21**, **28**, and **29** against a panel of kinases including CDK, PKC isoenzymes, and some additional ATP-dependent kinases (PKA, calmodulin K, and casein K; Table 2). Indeed, the macrocyclic bisindolylmaleimide **11** only showed very modest selectivities (3- to 4-fold) against selected PKC isoenzymes (PKCα and PKCθ), although it exhibited 1−2 orders of magnitude selectivity at GSK-3β versus CDK1, CDK2, and VEGF-R (vascular endothelial growth factor receptor-2) and was poorly active against the other ATP-dependent kinases tested (IC_{50} > 10 μM). Interestingly, in contrast to PKCγ, the mixed 7-azaindoleindolylmaleimide **21** exhibited better selectivity than bisindolylmaleimide **11** at GSK-3β over all of the kinases tested in Table 2. In other words, the addition of one nitrogen atom to one of the indole rings did increase the selectivity at GSK-3β over the other kinases. Consistently, the bis-7-azaindolylmaleimide **28** exhibited much greater selectivity at GSK-3β, i.e., 2−3 orders of magnitude, with only one lower selectivity observed (1−2 orders of magnitude against PKCβII). Meanwhile, bis-7-azaindolylmaleimide **29** exhibited high selectivity at GSK-3β against all kinases tested (Table 2).

To explore the degree of selectivity that these GSK-3β inhibitors can achieve, compounds **28** and **29** were evaluated against a broad panel of 51 protein kinases assays at UBI (Upstate Biotech Inc.). In the presence of 10 μM ATP, 10 μM **28** or 10 μM **29** inhibited GSK-3β kinase activity by 100% (Table 3). On the other hand, compound **28** only showed very weak inhibitory activity at the other 48 kinases except for the moderate inhibitions at PKCβII and RsK3 (ribosomal S6 kinase3). Remarkably, compound **29** exhibited very low activity against all of the other 50 kinases, therefore representing a GSK-3β "specific inhibitor".

Table 3. Activities at Protein Kinases Assays[a]

protein kinase	activity (% of control)		protein kinase	activity (% of control)	
	28	**29**		**28**	**29**
GSK3β (h)	0	0	MSK1 (h)	61	89
SAPK2b (h)	105	104	MKK7β (h)	129	132
PRK2 (h)	92	104	MKK4 (m)	110	107
PKCβII (h)	15	69	MAPK1 (h)	106	105
MAPK2 (m)	85	88	Lck (h)	194	174
JNK1α1 (h)	78	98	IKK a	100	98
CK1 (y)	84	89	IKK b	97	101
PRAK (h)	88	102	CSK	84	103
PKCα (h)	51	94	Syk	67	72
PKCγ (h)	77	96	Lyn	99	92
PKA (b)	88	94	Blk	90	96
PDK1 (h)	90	94	PKCθ	71	88
p70S6K (h)	92	93	CAMK IV	84	88
MKK6 (h)	87	85	CDK3/cycE	72	97
MEK1 (h)	94	100	CDK5/p35	82	105
MAPKAP-K2 (h)	97	85	CDK2/cyclinE	67	100
JNK3 (r)	54	81	CDK6/cyclin D3	97	97
JNK2α2 (h)	76	97	CDK7/cyclinH	85	86
Fyn (h)	92	95	Rsk3	21	63
cSRC (h)	90	89	IGF-1R	107	97
c-RAF (h)	91	97	IR	94	92
CK2 (h)	105	102	PKB β	93	97
CHK1 (h)	101	102	FGFR3	58	61
CaMKII (r)	108	70	PDGFR α	130	112
AMPK (r)	88	99	PDGFR β	84	86
PKBα (h)	97	102			

[a] Protein kinases were assayed with 10 μM **28** or **29** in the presence of 10 μM ATP. Activities are given as the mean percentage of that in control incubations (averages of duplicate determination). Assay details are described in the Experimental Section.

Cellular Activity

Among the multiple cellular processes in which GSK-3 has been implicated, the ability to phosphorylate and inhibit GS was the first regulation process that was discovered and is perhaps the best studied.[1] Therefore, the cell-based assay examining GS activation represents a direct functional assay to measure the cellular activity of GSK-3 inhibitors. Compounds **28**, **29**, and LiCl were tested for the ability to increase GS activity in human embryonic kidney (HEK293) cells. As described above, LiCl is a known inhibitor of GSK-3β. LiCl increases GS activity in isolated rat adipocytes and hepatocytes[33] and produces intracellular effects similar to the effects achieved by GSK-3 inhibition.[34,35] Both compound **28** (EC_{50} = 0.06 μM) and compound **29** (EC_{50} = 0.39 μM) exhibited much greater potency than LiCl (EC_{50} > 3000 μM) in the HEK293 cells (Table 4). The 6.5-fold difference in potencies between **28** and **29** in GS activity

Table 4. GS Activity in HEK293 Cells[a]

compd	$EC_{50} \pm$ SEM (μM)
28	0.06 ± 0.02
29	0.39 ± 0.01
LiCl	>3000

[a] Assay details were described in the Experimental Section.

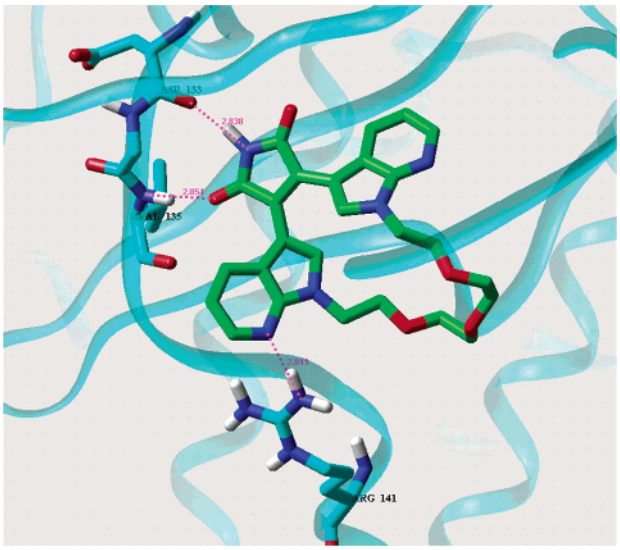

Figure 1. Illustration of the binding mode of compound **28** in the ATP-binding site of GSK-3β, suggested by the molecular docking studies. Compound **28** and its H-bonding parters (ASP133, VAL135, and ARG141) are represented in the stick model. The protein structure is described in the ribbon model. The key H-bonds between **28** and GSK-3β are indicated by the pink dotted lines, together with the bond lengths in angstroms. The atom color scheme is the following: hydrogen in gray; oxygen in red; nitrogen in blue; carbon on **28** in green; and carbon on GSK-3β in light blue.

compared to the similar IC_{50} values in GSK-3β (34 nM versus 48 nM) may be due to the differences in the species tested, i.e., human cells versus recombinant rabbit enzyme.

Molecular Docking Studies

Compounds **28** and **29** are very selective at GSK-3β, demonstrating only moderate or poor activity for other Ser/Thr kinases (Tables 2 and 3). In an attempt to rationalize this high selectivity, molecular docking studies were conducted for compound **28** based on the X-ray structure of GSK-3β (1h8f.pdb).[36] The binding mode derived from the best docking pose of **28** in the ATP binding site of GSK-3β is illustrated in Figure 1 (see Supporting Information for the coordinates of GSK-3β complexed with **28**). According to this model, compound **28** forms three H-bonds with GSK-3β when binding in its ATP-binding site. The first H-bond forms between the backbone carbonyl oxygen of ASP133 and the imide NH. The second H-bond is generated between the backbone nitrogen of VAL135 and the imide carbonyl oxygen. The third H-bond is formed between the side chain guanidine group of ARG141 and the azaindole nitrogen atom. The first two H-bonds that are set up with the backbone atoms are identical to those observed when staurosporine binds to various kinases such as CDK2,[37] LcK,[38] etc. The third H-bond with ARG141 appears to be unique to GSK-3β and provides an interesting model to explain the high GSK-3β selectivity observed for our 7-azaindolemaleimides.

The aligned sequences of several kinases selected from the UBI panel are listed in Figure 2. This alignment was adopted from the PKR (Protein Kinase Resource) database,[39] which includes hundreds of kinases whose sequences have been aligned by Hanks and Quinn.[40] It is clear from Figure 2 that the positively charged ARG141 is quite unique to GSK-3β, with many of the other kinases having a negatively charged residue at the same alignment position. Conceivably, the replacement of ARG141 by a negatively charged residue will not only disrupt the H-bonding with the azaindole nitrogen but also introduce an unfavorable repellent interaction with the lone-pair electrons on that nitrogen. This unique binding feature may explain why the bis-7-azaindoles (**28** and **29**) exhibit high selectivity at GSK-3β versus other kinases. Meanwhile, this model may also provide an explanation for the observed difference of selectivity between the mixed 7-azaindole (e.g., **21**) and the bis-7-azaindoles (e.g., **28** and **29**). Considering the overall symmetry of the structural scaffold, mixed 7-azaindoleindolylmaleimides may flip over (rotating 180° around the pseudosymmetrical axis) when binding to kinases with a negatively charged residue at the

```
                                                  141
GSK3β   ..... ---VYLNLVL DYVPE---TV Y | R | VARHYSRA KQT------- .....
PKCβII  ..... ---DRLYFMM EYVNG--GDL M | Y | HIQQVGR- ---------- .....
PKCγ    ..... ---DRLYFVM EYVTG--GDL M | Y | HIQQLGK- ---------- .....
CK1     ..... ---DYNVLVM DLLG---PSL E | D | LFNFCSRR ---------- .....
MEK1    ..... ---GEISICM EHMDG--GSL D | Q | VLKKAGR- ---------- .....
Fyn     ..... ---EPIYIVT EYMNK--GSL L | D | FLKDGEGR A--------- .....
cSRC    ..... ---EPIYIVT EYMSK--GSL L | D | FLKGETGK Y--------- .....
CHK1    ..... ---QWRWVVL EFAQG--GDL F | D | KIEPDVG- ---------- .....
Lck     ..... ---EPIYIIT EYMEN--GSL V | D | FLKTPSGI K--------- .....
CSK     ..... ---GGLYIVT EYMAK--GSL V | D | YLRSRGRS V--------- .....
Lyn     ..... ---EPIYIIT EYMAK--GSL L | D | FLKSDEGG K--------- .....
Blk     ..... ---EPIYIVT EYMAR--GCL L | D | FLKTDEGS R--------- .....
CAMK IV ..... ---TEISLVL ELVTG--GEL F | D | RIVEKGY- ---------- .....
CDK2    ..... ---NKLYLVF EFLHQ---DL K | K | FMDASALT G--------- .....
PDGFR b ..... ---GPIYIIT EYCRY--GDL V | D | YLHRNKHT FLQHHSDKRR .....
```

Figure 2. Sequence alignment of some kinases selected from PKR database to demonstrate the uniqueness of ARG141 at GSK-3β. The positive-charged residues are blue, while the negative-charged residues are red.

corresponding position of ARG141 at GSK-3β. Because of this behavior, the unfavorable repellent interaction caused by the azaindole nitrogen could be avoided.

As shown in Figure 2, there are also a few kinases with a neutral or even positively charged residue at the alignment position corresponding to ARG141 at GSK-3β. For example, CDK2 bears a positively charged LYS86 at that position. However, a close inspection of the X-ray structure of CDK2 and staurosporine complex (1aq1.pdb)[37] reveals that the positively charged side chain of LYS86 is actually oriented away from the ligand, and instead, the negatively charged side chain of ASP83 is the one closest to the 7-position of the indole ring of staurosporine. Therefore, we speculate that the selectivity difference of the 7-azaindolemaleimides observed may contribute significantly from the different interaction strengths with ARG141 at GSK-3β or the spatially equivalent residues at other kinases.

This binding model may also provide some insights into the GSK-3β potency trend observed for these maleimides (Table 1). Although compounds **11**, **21**, and **28** differ from one another in terms of the number of nitrogen atoms present in the indoles (atoms A and B, Table 1), they all exhibit similar submicromolar potencies. This could be partially explained by considering the effects of H-bonding and solvation/desolvation on the binding process, although it is difficult to predict the additive effects of these processes on ligand binding. In the case of bisindole **11**, which lacks the nitrogens at atoms A and B, no H-bond is formed with ARG141, but **11** does not need to break H-bonds with water at these positions and so does not pay a high desolvation penalty. On the other hand, bisazaindole **28**, containing nitrogens at both atoms A and B, may suffer a penalty from an unfavorable desolvation with water during the binding process, even though it forms a favorable H-bonding interaction with ARG141. For mixed-azaindole **21**, containing only one nitrogen at either atom A or B, there is a favorable tradeoff between H-bonding and desolvation effects, but **21** may have to pay the entropy price to orient itself with ARG141 during H-bond formation. A full discussion of the structure−activity relationships between these series requires a careful consideration of several factors, including H-bonding, solvation/desolvation effects, van der Waals forces, and electrostatic interactions, the subject of future computational studies.

Conclusion

Palladium-catalyzed cross-coupling reactions were used to synthesize the key intermediates **17** and **22** that resulted in the synthesis of novel macrocycles. All three macrocyclic series (bisindolyl-, mixed 7-azaindoleindolyl-, and bis-7-azaindolylmaleimides) were found to have submicromolar inhibitory potency at GSK-3β with various degrees of selectivity toward other protein kinases. To gain the inhibitory potency at GSK-3β, the ring sizes of these macrocycles may play a major role. For example, 19−22 member rings (**11**, **12**, **21**, **28**, and **29**) give the optimal potency. To achieve the selectivity at GSK-3β, the additional nitrogen atoms in the indole rings may contribute to a significant degree. For example, the mixed 7-azaindoleindolyl **21** exhibited 1−2 orders of magnitude selectivity at GSK-3β versus selected PKC isoenzymes and >2 orders of magnitude selectivity versus CDK1, CDK2, VEGF-R, PKA, calmodulin K, and casein K. On the other hand, the bis-7-azaindolylmaleimides **28** and **29** exhibited little or no inhibition to a panel of 50 protein kinases. Compound **29** almost behaved as a GSK-3β specific inhibitor. Both **28** and **29** displayed good potency in a GS assay. Molecular docking studies were conducted in an attempt to rationalize the GSK-3β selectivity of azaindolylmaleimides. The high selectivity, inhibitory potency, and cellular activities of **28** and **29** may render them as valuable pharmacological tools in elucidating the complex roles of GSK-3β in cell signaling pathways and the potential usage for the treatment of elevated level of GSK-3β involved diseases.

Experimental Section

Chemistry. ^{1}H NMR spectra were measured on a Bruker AC-300 (300 MHz) spectrometer using tetramethylsilane as an internal standard. Elemental analyses were obtained by Quantitative Technologies Inc. (Whitehouse, NJ), and the results were within 0.4% of the calculated values unless otherwise mentioned. Melting points were determined in open capillary tubes with a Thomas-Hoover apparatus and were uncorrected. The optical rotations were measured at 25 °C with an Autopol III polarimeter. Electrospray mass spectra (MS-ES) were recorded on a Hewlett-Packard 59987A spectrometer. High-resolution mass spectra (HRMS) were obtained on a Micromass Autospec E. spectrometer. The term "DMAP" refers to (dimethylamino)pyridine, "TFA" refers to trifluoroacetic acid, "NMP" refers to 1-methyl-2-pyrrolidinone, "DPPF" refers to 1,1′-bis(diphenylphosphino)ferrocene, "$Pd_2(dba)_3$" refers to tris(dibenzylideneacetone)dipalladium(0)/chloroform adduct, and "DPPA" refers to diphenylphosphorylazide.

General Procedure for the Synthesis of 6−9. 6,7,9,10,12,13-Hexahydro-21-methyl-5,23:14,19-dimetheno-20*H*-dibenzo[*h*,*n*]pyrrolo[3,4-*k*][1,4,7,16]dioxadiazacyclooctadecine-20,22(21*H*)-dione 6. To a suspension of Cs_2CO_3 (1.0 g, 3.2 mmol) and bisindolylmaleimide **1** (0.5 g, 1.5 mmol) in DMF (40 mL) at 100 °C was added bismesylate **2** (0.58 g, 1.9 mmol) in DMF (15 mL) via syringe pump for 3 h. After the addition was completed, the reaction mixture was cooled to 20 °C and stirred for another 3 h. The reaction mixture was diluted with $NH_4Cl_{(aq)}$ and extracted with CH_2Cl_2. The combined organic layer was washed with $NaCl_{(sat)}$, dried (Na_2SO_4), and concentrated. The product was purified by column chromatography (SiO_2, eluted with CH_2Cl_2/acetone) to give 0.29 g (43%) of **6** as a reddish-brown solid: ^{1}H NMR (300 MHz, $CDCl_3$) δ 7.79 (d, J = 8.0 Hz, 2 H), 7.41 (s, 2 H), 7.23 (m, 6 H), 4.20 (t, J = 4.5 Hz, 4 H), 3.68 (t, J = 4.5 Hz, 4 H), 3.34 (s, 4 H), 3.19 (s, 3 H); MS (ES) m/z 456 (M + H$^+$); FAB-HRMS (M + H$^+$) calcd for $C_{27}H_{26}N_3O_4$ 456.1923, found 456.1911.

6,7,9,10,12,13,15,16-Octahydro-24-methyl-5,26:17,22-dimetheno-23*H*-dibenzo[*k*,*q*]pyrrolo[3,4-*n*][1,4,7,10,19]-trioxadiazacycloheneicosine-23,25(24*H*)-dione 7. Replacing **2** with **3** and following the same procedure as in the preparation of **6** gave **7**: 62% yield; ^{1}H NMR (300 MHz, $CDCl_3$) δ 7.60 (s, 2 H), 7.33 (brt, J = 9.3 Hz, 4 H), 7.19 (t, J = 7.7 Hz, 2 H), 6.99 (t, J = 7.7 Hz, 2 H), 4.25 (t, J = 4.3 Hz, 4 H), 3.66 (m, 4 H), 3.18 (m, 11 H); MS (ES) m/z 500 (M + H$^+$). Anal. ($C_{29}H_{29}N_3O_5$·0.45H_2O) C, H, N.

6,7,9,10,12,13,15,16,18,19-Decahydro-27-methyl-5,29:20,25-dimetheno-26*H*-dibenzo[*n*,*t*]pyrrolo[3,4-*q*][1,4,7,10,-13,22]tetraoxadiazacyclotetracosine-26,28(27*H*)-dione 8. Replacing **2** with **4** and following the same procedure as in the preparation of **6** gave **8**: 56% yield; ^{1}H NMR (300 MHz, $CDCl_3$) δ 7.56 (s, 2 H), 7.32 (t, J = 7.5 Hz, 4 H), 7.21 (t, J = 7.1 Hz, 2 H), 7.01 (t, J = 7.7 Hz, 2 H), 4.22 (t, J = 4.9 Hz, 4 H), 3.72 (t, J = 4.9 Hz, 4 H), 3.47 (s, 4 H), 3.42 (m, 4 H), 3.34 (m, 4 H), 3.20 (s, 3 H); MS (ES) m/z 544 (M + H$^+$).

6,7,9,10,12,13,15,16,18,19,21,22-Dodecahydro-30-methyl-5,32:23,28-dimetheno-29*H*-dibenzo[*q*,*w*]pyrrolo[3,4-*t*][1,4,7,10,13,16,25]pentaoxadiazacycloheptacosine-29,31(30*H*)-dione 9. Replacing **2** with **5** and following the same procedure as in the preparation of **6** gave **9**: 21% yield; ^{1}H NMR (300 MHz, $CDCl_3$) δ 7.63 (s, 2 H), 7.40 (d, J = 8.1 Hz, 2 H), 7.17 (m, 4 H), 6.92 (t, J = 7.5 Hz, 2 H), 4.25 (t, J = 5.1 Hz, 4 H), 3.75 (t, J = 5.1 Hz, 4 H), 3.40 (m, 16 H), 3.20 (s, 3 H); MS (ES) m/z 588 (M + H$^+$); FAB-HRMS (M + H$^+$) calcd for $C_{33}H_{38}N_3O_7$ 588.2710, found 588.2711.

General Procedure for the Synthesis of 10−13. 6,7,9,10,12,13-Hexahydro-20*H*-5,23:14,19-dimetheno-5*H*-dibenzo[*h*,*n*]pyrrolo[3,4-*k*][1,4,7,16]dioxadiazacyclooctadecine-20,22(21*H*)-dione 10. A mixture of compound **6** (0.1 g, 0.22 mmol) in EtOH (1 mL) and 10 N KOH (0.22 mL, 2.2 mmol) was heated to a gentle reflux at 78 °C overnight. The reaction mixture was cooled to 0 °C and acidified with 1 N HCl. A dark-red precipitate was formed. The reaction mixture was extracted with CH_2Cl_2, and the combined organic layer was washed with $NaCl_{(sat)}$, dried (Na_2SO_4), and concentrated. The anhydride was obtained as a dark-red solid and used directly.

To a solution of anhydride in DMF (1.5 mL) was added a methanol solution (0.05 mL) containing HMDS (0.32 g, 1.97 mmol). The reaction mixture was heated at 80 °C for 6 h and cooled to 20 °C, and the solvent was removed under reduced pressure. The product was purified by column chromatography (SiO_2, eluted with CH_2Cl_2/acetone) to give 0.32 g (36%) of **10** as a dark-red solid after recrystallization from CH_2Cl_2/hexane: ^{1}H NMR (300 MHz, $CDCl_3$) δ 7.77 (d, J = 8.1 Hz, 2 H), 7.43 (s, 2 H), 7.26 (m, 6 H), 4.20 (m, 4 H), 3.69 (m, 4 H), 3.34 (s, 4 H); MS (ES) m/z 442 (M + H$^+$). Anal. ($C_{26}H_{23}N_3O_4$·1TFA·2H_2O) C, H, N.

6,7,9,10,12,13,15,16-Octahydro-23*H*-5,26:17,22-dimetheno-5*H*-dibenzo[*k*,*q*]pyrrolo[3,4-*n*][1,4,7,10,19]trioxadiazacycloheneicosine-23,25(24*H*)-dione 11. Replacing **6** with **7** and following the same procedure as in the preparation of **10** gave **11**: 80% yield; ^{1}H NMR (300 MHz, $CDCl_3$) δ 7.61 (s, 2 H), 7.34 (m, 5 H), 7.19 (t, J = 7.0 Hz, 2 H), 6.99 (t, J = 7.0 Hz, 2 H), 4.25 (t, J = 4.5 Hz, 4 H), 3.66 (t, J = 4.5 Hz, 4 H), 3.18 (s, 8 H); MS (ES) m/z 486 (M + H$^+$). Anal. ($C_{28}H_{27}N_3O_5$) C, H, N.

10,11,13,14,16,17,19,20,22,23-Decahydro-9,4:24,29-dimetheno-1*H*-dibenzo[*n*,*t*]pyrrolo[3,4-*q*][1,4,7,10,13,22]tetraoxadiazacyclotetracosine-1,3(2*H*)-dione 12. Replacing **6** with **8** and following the same procedure as in the preparation of **10** gave **12**: 55% yield; ^{1}H NMR (300 MHz, $CDCl_3$) δ 7.58 (s, 2 H), 7.42 (s, 1 H), 7.33 (m, 4 H), 7.23 (t, J = 6.6 Hz, 2 H), 7.02 (t, J = 7.0 Hz, 2 H), 4.22 (t, J = 4.9 Hz, 4 H), 3.72 (t, J = 4.9 Hz, 4 H), 3.48 (s, 4 H), 3.43 (m, 4 H), 3.35 (m, 4 H); MS (ES) m/z 530 (M + H$^+$). Anal. ($C_{30}H_{31}N_3O_6$·0.7H_2O) C, H, N.

10,11,13,14,16,17,19,20,22,23,25,26-Dodecahydro-9,4:27,32-dimetheno-1*H*-dibenzo[*q*,*w*]pyrrolo[3,4-*t*][1,4,7,10,13,16,25]pentaoxadiazacycloheptacosine-1,3(2*H*)-dione 13. Replacing **6** with **9** and following the same procedure as in the preparation of **10** gave **13**: 73% yield; ^{1}H NMR (300 MHz, $CDCl_3$) δ 7.64 (s, 2 H), 7.36 (s, 3 H), 7.17 (m, 4 H), 6.93 (t, J = 7.8 Hz, 2 H), 4.26 (t, J = 5.1 Hz, 4 H), 3.75 (t, J = 5.1 Hz, 4 H), 3.43 (m, 16 H); MS (ES) m/z 574 (M + H$^+$). Anal. ($C_{32}H_{35}N_3O_7$) C, H, N.

3-Trimethylstannanylpyrrolo[2,3-*b*]pyridine-1-carboxylic Acid *tert*-Butyl Ester 15. To a THF solution (15 mL) of 7-aza-1-(*tert*-butyloxycarbonyl)-3-iodoindole **14** (1.82 g, 5.3 mmol) at −78 °C was added trimethyltin chloride (26.5 mL, 1 M in THF, 26.5 mmol) under nitrogen. After 10 min, *n*-BuLi (10 mL, 1.6 M in hexane, 16 mmol) was added dropwise at −78 °C and the reaction mixture was allowed to warm to 20 °C overnight. Water (4 mL) was added, and the solvent was removed under reduced pressure. The residue was diluted with hexane (250 mL), and the organic layer was washed with water, dried (Na_2SO_4), and concentrated. The product was purified by column chromatography (SiO_2) to give 1.198 g (60%) of organostannane **15** as an oil: ^{1}H NMR (300 MHz, $CDCl_3$) δ 8.45 (d, J = 4.9 Hz, 1 H), 7.77 (d, J = 7.6 Hz, 1 H), 7.48 (s, 1 H), 7.13 (dd, J = 7.7, 4.8 Hz, 1 H), 1.65 (s, 9 H), 0.36 (m, 9 H); MS (ES) m/z 405 (M + Na).

3-(1*H*-Indol-3-yl)-1-methyl-4-(1*H*-pyrrolo[2,3-*b*]pyridin-3-yl)pyrrole-2,5-dione 17. A mixture of chloroindolylmaleimide **16** (0.929 g, 3.57 mmol), organostannane **15** (1.59 g, 3.57 mmol), lithium chloride (2.06 g, 49 mmol), and dichlorobis(triphenylphosphine)palladium(II) (0.34 g, 0.49 mmol) in toluene (45 mL) was heated at 95 °C under nitrogen overnight. The reaction mixture was concentrated, CH_2Cl_2 (7.5 mL) and TFA (2.5 mL) were added, and the mixture was stirred at 20 °C for 2.5 h and concentrated under reduced pressure. The reaction mixture was purified by column chromatography (SiO_2, eluted with CH_2Cl_2/acetone) to give a mixture of an orange product and 7-azaindole. The crude product was triturated with ether to remove 7-azaindole, and an orange solid of **17** (0.376 g, 31%) was collected through filtration: ^{1}H NMR (300 MHz, acetone-d_6) δ 8.05 (d, J = 4.0 Hz, 1 H), 7.88 (s,1 H), 7.85 (s,1 H), 7.35 (d, J = 8.2 Hz, 1 H), 7.23 (d, J = 8.1 Hz, 1 H), 6.97 (t, J = 7.8 Hz, 1 H), 6.68 (m, 3 H), 3.13 (s, 3 H); FAB-HRMS (M + H$^+$) calcd for $C_{20}H_{15}N_4O_2$ 343.1195, found 343.1205.

General Procedure for the Synthesis of 18 and 19. 6,7,9,10,12,13-Hexahydro-21-methyl-5,23:14,19-dimetheno-20*H*-pyrido[2,3-*k*]pyrrolo[3,4-*n*][4,7,1,10]benzodioxadiazacyclooctadecine-20,22(21*H*)-dione 18. To a slurry of **17** (246 mg, 0.72 mmol) and Cs_2CO_3 (394 mg, 1.2 mmol) in DMF (20 mL) at 100 °C was added bismesylate **2** (220 mg, 0.72 mmol) in DMF (10 mL) in 2 h with a syringe pump. The reaction mixture was heated at 100 °C for 20 h, cooled to 20 °C, and concentrated under reduced pressure. Water was added and the residue was extracted with CH_2Cl_2, dried (Na_2SO_4), and concentrated. The product was purified by column chromatography (SiO_2, eluted with CH_2Cl_2/acetone) to give 160 mg (49%) of **18** as a brick-red solid: ^{1}H NMR (300 MHz, $CDCl_3$) δ 8.33 (d, J = 4.8 Hz, 1 H), 8.25 (d, J = 7.0 Hz, 1 H), 7.65 (d, J = 7.8 Hz, 1 H), 7.59 (s, 1 H), 7.45 (s, 1 H), 7.34 (d, J = 8.1 Hz, 1 H), 7.26 (m, 1 H), 7.16 (m, 2 H), 4.37 (t, J = 4.5 Hz, 2 H), 4.27 (t, J = 4.7 Hz, 2 H), 3.76 (t, J = 4.8 Hz, 2 H), 3.69 (t, J = 4.5 Hz, 2 H), 3.38 (m, 4 H), 3.20 (s, 3 H); MS (ES) m/z 457(M + H$^+$). Anal. ($C_{26}H_{24}N_4O_4$·1.5H_2O) C, H, N.

6,7,9,10,12,13,15,16-Octahydro-24-methyl-5,26:17,22-dimetheno-23*H*-pyrido[2,3-*n*]pyrrolo[3,4-*q*][4,7,10,1,13]benzotrioxadiazacycloheneicosine-23,25(24*H*)-dione 19. Replacing **2** with **3** and following the same procedure as in the preparation of **18** gave **19**: 27% yield; ^{1}H NMR (300 MHz, $CDCl_3$) δ 8.34 (d, J = 3.7 Hz, 1 H), 8.05 (d, J = 7.1 Hz, 1 H), 7.78 (s, 1 H), 7.62 (s, 1 H), 7.40 (d, J = 8.2 Hz, 1 H), 7.14 (m, 2 H), 6.90 (m, 2 H), 4.44 (m, 2 H), 4.35 (m, 2 H), 3.77 (m, 2 H), 3.60 (m, 2 H), 3.38 (m, 4 H), 3.20 (s, 3 H), 3.02 (m, 4 H); MS (ES) m/z 501 (M + H$^+$). Anal. ($C_{28}H_{28}N_4O_5$·0.5H_2O) C, H, N.

General Procedure for the Synthesis of 20 and 21. 6,7,9,10,12,13-Hexahydro-20*H*-5,23:14,19-dimetheno-5*H*-pyrido[2,3-*k*]pyrrolo[3,4-*n*][4,7,1,10]benzodioxadiazacyclooctadecine-20,22(21*H*)-dione 20. A mixture of **18** (124 mg, 0.271 mmol) and 10 N KOH (0.77 mL, 7.7 mmol) in ethanol (4.2 mL) was heated to a gentle reflux at 78 °C overnight. The reaction mixture was cooled in an ice bath. Then 12 N HCl (2.3 mL) and CH_2Cl_2 (3 mL) were added, and the reaction mixture was stirred at 0 °C for 20 min. The reaction mixture was partitioned between CH_2Cl_2 (40 mL) and $NaHCO_{3(aq)}$ (40 mL). The separated aqueous layer was extracted with CH_2Cl_2. The combined organic layers were dried (Na_2SO_4) and concentrated under reduced pressure to give the crude anhydride (120 mg).

To a solution of the anhydride in DMF (7 mL) was added a methanol solution (0.2 mL) containing HMDS (1.19 g, 7.46 mmol). The reaction mixture was heated overnight at 80 °C. The cooled reaction mixture was concentrated under reduced pressure, and the product was purified by column chromatography (SiO_2, eluted with CH_2Cl_2/acetone) to give 39 mg (33%) of **20** as an orange solid: ^{1}H NMR (300 MHz, DMSO-d_6) δ 11.05 (bs, 1 H), 8.29 (d, J = 3.3 Hz, 1 H), 8.11 (d, J = 7.9 Hz, 1 H), 7.74 (s, 1 H), 7.62 (s, 1 H), 7.54 (d, J = 8.4 Hz, 2 H), 7.18 (m, 2 H), 7.05 (t, J = 7.8 Hz, 1 H), 4.36 (m, 4 H), 3.68 (m, 4 H),

3.39 (m, 4 H); FAB-HRMS (M + H^+) calcd for $C_{25}H_{23}N_4O_4$ 443.1719, found 443.1713.

6,7,9,10,12,13,15,16-Octahydro-23*H*-5,26:17,22-dimetheno-5*H*-pyrido[2,3-*n*]pyrrolo[3,4-*q*][4,7,10,1,13]-benzotrioxadiazacycloheneicosine-23,25(24*H*)-dione 21. Replacing **18** with **19** and following the same procedure as in the preparation of **20** gave **21**: 83% yield; ^{1}H NMR (300 MHz, acetone-d_6) δ 9.66 (brs, 1 H), 8.31 (d, J = 4.0 Hz, 1 H), 7.98 (d, J = 8.1 Hz, 1 H), 7.83 (s, 1 H), 7.64 (s, 1 H), 7.56 (d, J = 8.4 Hz, 1 H), 7.12 (m, 2 H), 6.87 (d, J = 4.0 Hz, 2 H), 4.43 (m, 4 H), 3.83 (m, 2 H), 3.61 (m, 2 H), 3.33 (m, 4 H), 3.07 (s, 4 H). Anal. ($C_{27}H_{26}N_4O_5$·0.7 H_2O) C, H, N.

1-Methyl-3,4-bis(1*H*-pyrrolo[2,3-*b*]pyridine-3-yl)pyrrole-2,5-dione 22. A mixture of **15** (185 mg, 0.486 mmol), 2,3-dichloro-*N*-methylmaleimide (29 mg, 0.162 mmol), $PdCl_2(PPh_3)_2$ (5.4 mg, 0.0077 mmol), and LiCl (32 mg, 0.77 mmol) in anhydrous toluene (2 mL) was stirred at 95 °C overnight. The solvent was removed under reduced pressure. The product was purified by column chromatography (SiO_2) to give 23 mg (41%) of **22** as an orange-red solid: ^{1}H NMR (300 MHz, DMSO-d_6) δ 12.35 (s, 2 H), 8.12 (brd, J = 3.9 Hz, 2 H), 7.92 (s, 2 H), 7.08 (d, J = 7.7 Hz, 2 H), 6.73 (m, 2 H), 3.06 (s, 3 H); MS (ES) m/z 344 (M + H^+). Anal. ($C_{19}H_{13}N_5O_2$·2.2TFA·0.5H_2O) C, H, N.

General Procedure for the Synthesis of 23−26. 6,7,9,10,12,13-Hexahydro-21-methyl-5,23:14,19-dimetheno-20*H*-dipyrido[2,3-*h*:3′,2′-*n*]pyrrolo[3,4-*k*][1,4,7,16]dioxadiazacyclooctadecine-20,22(21*H*)-dione 23. To a suspension of Cs_2CO_3 (115 mg, 0.35 mmol) and bis-7-azaindolylmaleimide **22** (41 mg, 0.12 mmol) in DMF (6 mL) at 100 °C was added bismesylate **2** (54 mg, 0.18 mmol) in DMF (1.5 mL) via syringe pump for 3 h. After the addition was completed, the reaction mixture was cooled to 20 °C and stirred for another 15 h. The reaction mixture was diluted with $NH_4Cl_{(aq)}$ and extracted with EtOAc. The combined organic layer was washed with $NaCl_{(sat)}$, dried (Na_2SO_4), and concentrated. The product was purified by column chromatography (SiO_2, eluted with CH_2Cl_2/acetone) to give 25 mg (67%) of **23** as an orange solid: ^{1}H NMR (300 MHz, $CDCl_3$) δ 8.35 (dd, J = 4.7, 1.4 Hz, 2 H), 8.11 (dd, J = 8.0, 1.5 Hz, 2 H), 7.63 (s, 2 H), 7.12−7.16 (dd, J = 8.0, 4.7 Hz, 2 H), 4.42 (t, J = 4.6 Hz, 4 H), 3.77 (t, J = 4.8 Hz, 4 H), 3.45 (s, 4 H), 3.20 (s, 3 H); MS (ES) m/z 458 (M + H^+).

6,7,9,10,12,13,15,16-Octahydro-24-methyl-5,26:17,22-dimetheno-23*H*-dipyrido[2,3-*k*:3′,2′-*q*]pyrrolo[3,4-*n*]-[1,4,7,10,19]trioxadiazacyclohenicosine-23,25(24*H*)-dione 24. Replacing **2** with **3** and following the same procedure as in the preparation of **23** gave **24**: 31% yield; ^{1}H NMR (300 MHz, $CDCl_3$) δ 8.32 (m, 2 H), 7.80 (s, 2 H), 7.61 (d, J = 7.1 Hz, 2 H), 6.99 (m, 2 H), 4.50 (t, J = 4.5 Hz, 4 H), 3.71 (t, J = 4.5 Hz, 4 H), 3.22 (m, 11 H); MS (ES) m/z 502 (M + H^+); FAB-HRMS (M + H^+) calcd for $C_{27}H_{28}N_5O_5$ 502.2090, found 502.2110.

6,7,9,10,12,13,15,16,18,19-Decahydro-27-methyl-5,29:20,25-dimetheno-26*H*-dipyrido[2,3-*n*:3′,2′-*t*]pyrrolo[3,4-*q*]-[1,4,7,10,13,22]tetraoxadiazacyclotetracosine-26,28,(27*H*)-dione 25. Replacing **2** with **4** and following the same procedure as in the preparation of **23** gave **25**: 39% yield; ^{1}H NMR (300 MHz, $CDCl_3$) δ 8.32 (m, 2 H), 7.80 (s, 2 H), 7.57 (dd, J = 8.0, 1.5 Hz, 2 H), 7.00 (m, 2 H), 4.44 (t, J = 4.6 Hz, 4 H), 3.77 (t, J = 4.6 Hz, 4 H), 3.43 (m, 12 H), 3.20 (s, 3 H); MS (ES) m/z 546 (M + H^+); FAB-HRMS (M + H^+) calcd for $C_{29}H_{32}N_5O_6$ 546.2353, found 546.2372.

6,7,9,10,12,13,15,16,18,19,21,22-Dodecahydro-30-methyl-5,32:23,28-dimetheno-29*H*-dipyrido[2,3-*q*:3′,2′-*w*]pyrrolo-[3,4-*t*][1,4,7,10,13,16,25]pentaoxadiazacycloheptacosine-29,31(30*H*)-dione 26. Replacing **2** with **5** and following the same procedure as in the preparation of **23** gave **26**: 24% yield; ^{1}H NMR (300 MHz, $CDCl_3$) δ 8.27 (m, 2 H), 7.89 (s, 2 H), 7.42 (dd, J = 9.4, 1.4 Hz, 2 H), 6.89 (m, 2 H), 4.47 (t, J = 4.8 Hz, 4 H), 3.80 (t, J = 4.8 Hz, 4 H), 3.46 (s, 8 H), 3.41 (s, 8 H), 3.20 (s, 3 H); MS (ES) m/z 590 (M + H^+); FAB-HRMS (M + H^+) calcd for $C_{31}H_{36}N_5O_7$ 590.2615, found 590.2624.

General Procedure for the Synthesis of 27−30. 6,7,9,10,12,13-Hexahydro-20*H*-5,23:14,19-dimetheno-5*H*-dipyrido[2,3-*h*:3′,2′-*n*]pyrrolo[3,4-*k*][1,4,7,16]dioxadiazacyclooctadecine-20,22(21*H*)-dione 27. A mixture of **23** (47 mg, 0.10 mmol) and 10 N KOH (0.1 mL) in ethanol (2 mL) was heated to a gentle reflux at 78 °C overnight. The reaction mixture was cooled in an ice bath and acidified with 1 N HCl. The reaction mixture was partitioned between CH_2Cl_2 (15 mL) and $NaHCO_{3(aq)}$ (15 mL). The separated aqueous layer was extracted with CH_2Cl_2. The combined organic layers were dried (Na_2SO_4) and concentrated under reduced pressure to give the crude anhydride.

To a solution of the anhydride in DMF (1 mL) was added a methanol solution (0.06 mL) containing HMDS (0.25 mL, 1 mmol). The reaction mixture was heated at 80 °C for 6 h and cooled to 20 °C, and the solvent was removed under reduced pressure. The product was purified by column chromatography (SiO_2, eluted with CH_2Cl_2/acetone) to give 27 mg (60%) of **27** as a red solid: ^{1}H NMR (300 MHz, $CDCl_3$) δ 8.35 (dd, J = 4.7, 1.5 Hz, 2 H), 8.10 (dd, J = 8.0, 1.5 Hz, 2 H), 7.65 (s, 2 H), 8.12−8.17 (dd, J = 8.0, 4.7 Hz, 2 H), 4.41 (t, J = 4.9 Hz, 4 H), 3.77 (t, J = 4.9 Hz, 4 H), 3.44 (s, 4 H); MS (ES) m/z 444 (M + H^+). Anal. ($C_{24}H_{21}N_5O_4$·0.74H_2O) C, H, N.

6,7,9,10,12,13,15,16-Octahydro-23*H*-5,26:17,22-dimetheno-5*H*-dipyrido[2,3-*k*:3′,2′-*q*]pyrrolo[3,4-*n*]-[1,4,7,10,19]trioxadiazacyclohenicosine-23,25(24*H*)-dione 28. Replacing **23** with **24** and following the same procedure as in the preparation of **27** gave **28**: 74% yield; ^{1}H NMR (300 MHz, $CDCl_3$) δ 8.32 (d, J = 4.3 Hz, 2 H), 7.81 (s, 2 H), 7.60 (d, J = 7.8 Hz, 2 H), 7.49 (s, 1 H), 7.00 (m, 2 H), 4.50 (t, J = 4.5 Hz, 4 H), 3.71 (t, J = 4.5 Hz, 4 H), 3.23 (m, 8 H); MS (ES) m/z 488 (M + H^+). Anal. ($C_{22}H_{25}N_5O_5$·0.7H_2O) C, H, N.

10,11,13,14,16,17,19,20,22,23-Decahydro-9,4:24,29-dimetheno-1*H*-dipyrido[2,3-*n*:3′,2′-*t*]pyrrolo[3,4-*q*]-[1,4,7,10,13,22]tetraoxadiazacyclotetracosine-1,3(2*H*)-dione 29. Replacing **23** with **25** and following the same procedure as in the preparation of **27** gave **29**: 41% yield; ^{1}H NMR (300 MHz, $CDCl_3$) δ 8.32 (d, J = 4.5 Hz, 2 H), 7.83 (s, 2 H), 7.66 (s, 1 H), 7.57 (d, J = 7.9 Hz, 2 H), 6.99 (m, 2 H), 4.45 (t, J = 4.7 Hz, 4 H), 3.77 (t, J = 4.7 Hz, 4 H), 3.45 (m, 12 H); MS (ES) m/z 532 (M + H^+). Anal. ($C_{28}H_{29}N_5O_6$·0.25H_2O) C, H, N.

10,11,13,14,16,17,19,20,22,23,25,26-Dodecahydro-9,4:27,-32-dimetheno-1*H*-dipyrido[2,3-*q*:3′,2′-*w*]pyrrolo[3,4-*t*]-[1,4,7,10,13,16,25]pentaoxadiazacycloheptacosine-1,3-(2*H*)-dione 30. Replacing **23** with **26** and following the same procedure as in the preparation of **27** gave **30**: 62% yield; ^{1}H NMR (300 MHz, $CDCl_3$) δ 8.29 (m, 2 H), 7.90 (s, 2 H), 7.80 (s, 1 H), 7.42 (dd, J = 8.0, 1.4 Hz, 2 H), 6.90 (m, 2 H), 4.48 (t, J = 4.9 Hz, 4 H), 3.81 (t, J = 4.9 Hz, 4 H), 3.47 (s, 8 H), 3.43 (s, 8 H); MS (ES) m/z 576 (M + H^+). Anal. ($C_{30}H_{33}N_5O_7$·1.5H_2O) C, H, N.

Biology. GSK-3β Kinase Assay. Compounds were tested for the ability to inhibit recombinant rabbit GSK-3β (New England Biolabs) using the following protocol. Protein phosphatase inhibitor-2 (PPI-2, Calbiochem) phosphorylation was measured using a standard filtration assay (MultiScreen-DV/Millipore). Briefly, the test compounds were added to a reaction mixture containing PPI-2 (45 ng), GSK-3β (0.75 units), and ^{33}P-ATP (1 μCi) in 50 mM Tris-HCl (pH 8.0), 10 mM $MgCl_2$, 0.1% BSA, 1 mM DTT, and 100 μM activated sodium orthovanadate. The total ATP concentration was 25 μM. After 90 min of incubation at 30 °C, the phosphorylated PPI-2 was precipitated using one volume of 20% trichloroacetic acid (TCA). Filter plates were subsequently washed with 10% TCA, and radioactivity was quantified using a TopCount scintillation counter (Packard). Results were expressed as IC_{50} values ± SEM from at least 3 separate experiments done in duplicate with 6−10 different concentrations tested.

PKCα, PKCγ, and PKCβII Assays. Compounds were tested for the ability to inhibit recombinant human PKCα, PKCγ, and PKCβII using the following protocol. Histone H1 phosphorylation was measured using a standard filtration

assay. Briefly, the test compounds were added to a reaction mixture containing histone H1 (0.1 mg/mL), the PKC isoform (5−10 mU), and ^{33}P-ATP (1 μCi) in 50 mM Hepes (pH 7.4), 0.03% Triton X-100, 0.1 mM $CaCl_2$, 10 mM magnesium acetate, 0.1 mg/mL phosphatidylserine, and 10 μg/mL diacylglycerol. The total ATP concentration was 10 μM. After 40 min of incubation at room temperature, the reaction was stopped by the addition of 5 μL of a 3% phosphoric acid solution. The reaction mix was then spotted onto a P30 filtermat, and the filters were washed three times for 5 min with 75 mM phosphoric acid. The filtermat was then washed one time with MeOH and dried prior to counting. Results were expressed as IC_{50} values ± SEM from at least 3 separate experiments done in duplicate with 6−10 different concentrations tested.

PKCθ Assay. Compounds were tested for the ability to inhibit recombinant human PKCθ using the following protocol. Histone H1 phosphorylation was measured using a standard filtration assay. Briefly, the test compounds were added to a reaction mixture containing histone H1 (0.1 mg/mL), PKCθ (5−10 mU), and ^{33}P-ATP (1 μCi) in 8 mM MOPS (pH 7.0), 0.2 mM EDTA, and 10 mM magnesium acetate. The total ATP concentration was 10 μM**.** After 40 min of incubation at room temperature, the reaction was stopped by the addition of 5 μL of a 3% phosphoric acid solution. The reaction mix was then spotted onto a P30 filtermat, and the filters were washed three times for 5 min with 75 mM phosphoric acid. The filtermat was then washed one time with MeOH and dried prior to counting. Results were expressed as IC_{50} values ± SEM from at least 3 separate experiments done in duplicate with 6−10 different concentrations tested.

CDK1, CDK2, VEGF-R, PKA, Calmdulin K, and Casein K Assays. A kinase reaction mixture was prepared containing 50 mM Tris-HCl (pH 8.0), 10 mM $MgCl_2$, 0.1 mM Na_3VO_4, 1 mM DTT, 10 μM ATP, 0.025 μM biotinylated peptide substrate, and 0.2 μCi/ well ^{33}P-ATP (2000−3000 Ci/mmol). An amount of 70 μL of the kinase reaction mixture was dispensed into each well of a streptavidin-coated Flashplate (catalog no. SMP103, NEN, Boston, MA). Then 1 μL of test compound stock in 100% DMSO was added to the wells, resulting in a final concentration of 1% DMSO in the reaction mixture with a 100 μL final reaction volume. Next, kinase enzyme was diluted in 50 mM Tris-HCl (pH 8.0) and 0.1% BSA at a concentration of 1−5 ng/μL, and 30 μL (30−150 ng of enzyme) was added to each well to initiate the reaction. The reaction mixture was incubated for 1 h at 30 °C, and the reaction was terminated by aspirating the reaction mixture from the plate and washing the wells twice with PBS containing 100 mM EDTA. The biotinylated peptide substrate became immobilized on the Flashplate, and the incorporation of ^{33}P-ATP was measured by reading the plate on a scintillation counter. Inhibition of the enzymatic activity due to the compound was measured by observing the reduced amount of ^{33}P-ATP incorporated into the immobilized peptide relative to that for untreated controls. Reaction conditions varied slightly depending on the protein kinase being assayed. For the calmodulin kinase enzyme, the reaction mixture contained 2 mM $CaCl_2$ and 2.4 μM calmodulin. Biotinylated peptide substrates were as follows: CDK1 and -2 (biotin-KTPKKAKKPKTPKKAKKL-amide), VEGF-R2 (biotin-KHKKLAEGSAYEEV-amide), protein kinase A (biotin-GRTGRRNSI-amide), casein kinase 1 (biotin-KRRRALS(phospho)VASLPGL-amide), and calmodulin kinase 2 (biotin-KKALRRQETVDAL-amide). Results were expressed as IC_{50} values ± SEM from at least 3 separate experiments done in duplicate with 6−10 different concentrations tested.

Protein Kinase Selectivity Panel (Upstate Biotech Inc.). Protein kinase selectivity assays were performed as previously described.[41] Briefly, protein kinases were assayed for their ability to phosphorylate the appropriate peptide/protein substrates in the presence of 10 μM compound. Assays were done using 10 μM ATP, and the results were linear with respect to time.

Glycogen Synthase Assay. Compounds were tested for the ability to increase glycogen synthase (GS) activity in living cells (HEK293 cells). To do this, cell extracts were prepared from cells treated with compounds or vehicle and GS activity was measured using a modified protocol.[17] Briefly, cells were serum (and glucose) starved for 3 h and treated with the appropriate compounds for 90 min at 37 °C. Cells were then washed, scraped, and collected by centrifugation prior to lysis using three freeze−thaw cycles. Lysates were then clarified by centrifugation, and the supernatants were assayed for GS activity. To do this, ^{14}C-UDP glucose incorporation into glycogen was measured in the absence or presence of glucose 6-phosphate. The EC_{50} for GS activation was then determined and compared with lithium. Results were expressed as EC_{50} values ± SEM from at least 3 separate experiments done in duplicate with 6−10 different concentrations tested.

Molecular Docking Procedures. The X-ray structure of unbound GSK-3β (1h8f.pdb)[36] was used as the target structure for docking. Its ATP-binding site was determined by superimposition onto the X-ray structure of the CDK2 and staurosporine complex (1aq1.pdb)[37] by SYBYL/Bioploymer software,[42] which uses the Needleman and Wunsch algorithm for the pairwise alignment of sequences,[43] and defined as the spatial region that staurosporine occupies after alignment.

Conformational searching was first conducted for compound **28**, using the MCMM (Monte Carlo multiple minimum)[44] method implemented in MacroModel,[45] leading to 1811 low-energy and unique conformers. The cutoff of the energy window was set as 50 kJ/mol, and the Monte Carlo steps were set to 5000 times. Conformational structures were not considered unique unless the least-squares superimposition of heavy atoms found one or more pairs of equivalent atoms separated by more than 0.25 Å. All of the 1811 conformational structures were then individually docked into the ATP binding site of GSK-3β, using the program Glide.[46] Both the compound **28** conformational structure and the GSK-3β protein structure were held rigid during the docking. The docking poses were evaluated by the empirical scoring function GlideScore.[47] The GSK-3β structure complexed with the best-scoring pose of compound **28** was further optimized by full energy minimization and then treated as the binding structure of GSK-3β and compound **28** (Supporting Information).

All the molecular mechanism calculations were done with the program MacroModel,[45] using the OPLS_AA force field.[48] The effect of aqueous solution was treated by the GB/SA model.[49]

Acknowledgment. We thank Thomas Rano for helping to purify some of the products via HPLC, and we thank Virginia Pulito, Robert Gruninger, and Angel Fuentes-Pesquera for testing some of the compounds in kinase assays.

Appendix

Abbreviations. AMPK, AMP-activated protein kinase; Blk, B lymphocyte kinase; CHK1, checkpoint kinase 1; CK1, casein kinase 1; CK2, casein kinase 2; CAMKII, calmodulin-dependent protein kinase II; CAMKIV, calmodulin-dependent protein kinase IV; CDK2/cyclinE, cycline-dependent protein kinase 2; CDK3/cycE, cyclin-dependent protein kinase 3; CDK5/p35, cyclin-dependent protein kinase 5; CDK6/cyclin D3, cyclin-dependent protein kinase 6; CDK7/cyclin H, cyclin-dependent protein kinase 7; CSK, carboxy-terminal Src kinase; FGFR3, FGF receptor kinase 3; Fyn, product of fyn protooncogene; GSK-3β, glycogen synthase kinase-3β; IGF-1R, insulin-like growth factor-1 receptor kinase; IKK, IκB kinase; IR, insulin receptor kinase; JNK1α1, c-Jun N-terminal kinase 1α1; JNK2α2, c-Jun N-terminal kinase 2α2; JNK3, c-Jun N-terminal kinase 3; Lck, lymphocyte kinase; Lyn, Lck/Yes-related tyrosine kinase; MAPK1, mitogen-activated protein kinase 1; MAPK2, mitogen-activated protein kinase 2; MAPKAP-

K2, MAPK-activated protein kinase 2; MEK1, MAPK/ERK kinase 1; MKK4, MAPK kinase 4; MKK6, MAPK kinase 6; MKK7β, MAPK kinase 7β; MSK1, mitogen- and stress-activated protein kinase 1; P70S6K, p70 ribosomal protein S6 kinase; PDGFR, platelet-derived growth factor receptor; PDK1, 3-phosphoinositide-dependent protein kinase 1; PKA, camp-dependent protein kinase; PKBα, protein kinase B α (also called Akt); PKBβ, protein kinase B β; PKC, protein kinase C; PRAK, p38-regulated/activated kinase; PRK2, protein kinase C-related protein kinase 2; c-Raf, cellular product of raf protooncogene; RsK, ribosomal S6 kinase; SAPK2b, stress-activated protein kinase 2b (also known as p38β2); c-SRC, cellular product of src oncogene; Syk, splenic tyrosine kinase; h, human; r, rat; m, mouse; b, bovine; y, yeast.

Supporting Information Available: Coordinates of GSK-3β complexed with compound **28.** This material is available free of charge via the Internet at http://pubs.acs.org.

References

(1) Embi, N.; Rylatt, D. B.; Cohen, P. Glycogen synthase kinase-3 from rabbit skeletal muscle: separation from cAMP-dependent protein kinase and phosphorylase kinase. *Eur. J. Biochem*. **1980**, *107*, 519−527.

(2) Welsh, G. I.; Proud, C. G. Glycogen synthase kinase-3 is rapidly inactivated in response to insulin and phosphorylates eukaryotic initation factor eIF-2B. *Biochem. J*. **1993**, *294*, 625−629.

(3) Woodgett, J. R. Molecular cloning and expression of glycogen synthase kinase-3/factor A. *EMBO J*. **1990**, *9*, 2431−2438.

(4) Grimes, C. A.; Jope, R. S. The multifaceted roles of glycogen synthase kinase 3β in cellular signaling. *Prog. Neurobiol*. **2001**, *65*, 391−426.

(5) Eldar-Finkelman, H. Glycogen synthase kinase 3: an emerging therapeutic target. *Trends Mol. Med*. **2002**, *8* (3), 126−132.

(6) Kaidanovich, O.; Eldar-Finkelman, H. The role of glycogen synthase kinase-3 in insulin resistance and type 2 diabetes. *Expert Opin. Ther. Targets* **2002**, *6* (5), 555−561.

(7) (a) Lovestone, S.; Reynolds, C. H.; Latimer, D.; Davis, D. R.; Anderton, B. H.; Gallo, J.-M.; Hanger, D.; Mulot, S.; Marquardt, B.; Stabel, S.; Woodgett, J. R.; Miller, C. C. J. Alzheimer's disease-like phosphorylation of the microtubule-associated protein tau by glycogen synthase kinase-3 in transfected mammalian cells. *Curr. Biol*. **1994**, *4*, 1077−1086. (b) Pap, M.; Cooper, G. M. Role of glycogen synthase kinase-3 in the phosphatidylinositol 3-kinase/akt cell survival pathway. *J. Biol. Chem*. **1998**, *273*, 19929−19954. (c) Lucas, J. J.; Hernandez, F.; Gomez-Ramos, P.; Moran, M. A.; Hen, R.; Avila, J. Decreased nuclear β-catenin, tau hyperphosphorylation and neurodegeneration in GSK-3β conditional transgenic mice. *EMBO J*. **2001**, *20*, 27−39.

(8) Cross, D.; Cubert, A. A.; Chalmers, K. A.; Facci, L.; Skaper, S. D.; Reith, A. D. Selective small molecule inhibitors of glycogen synthase kinase-3 activity protects primary neurons from death. *J. Neurochem*. **2001**, *77*, 94−102.

(9) Castro, A.; Martinez, A. Inhibition of tau phosphorylation: a new therapeutic strategy for the treatment of Alzheimer's disease and other neurodegenerative disorders. *Expert Opin. Ther. Pat.* **2000**, *10*, 1519−1527.

(10) Phiel, C. J.; Klein, P. S. Molecular targets of lithium action. *Annu. Rev. Pharmacol. Toxicol*. **2001**, *41*, 789−813.

(11) Hoeflich, K. P.; Luo, J.; Rubie, E. A.; Tsao, M.-S.; Jin, O.; Woodgett, J. R. Requirement for glycogen synthase kinase-3β in cell survival and NF-κB activation. *Nature* **2000**, *406*, 86−90.

(12) Bray, A. M.; Schultz, P.; Ring, D. B.; Harrison, S. D. Purine inhibitors of glycogen synthase kinase (GSK3). Chiron Corp. Patent WO9816528, 1998.

(13) Dorronsoro, I.; Castro, A.; Martinez, A. Inhibitors of glycogen synthase kinase-3: future therapy for unmet medical needs? *Expert Opin. Ther. Pat.* **2002**, *12* (10), 1527−1536.

(14) Martinez, A.; Castro, A.; Dorronsoro, I.; Alonso, M. Glycogen synthase kinase 3 (GSK-3) inhibitors as new promising drugs for diabetes, neurodegeneration, cancer, and inflammation. *Med. Res. Rev.* **2002**, *22* (4), 373−384.

(15) Martinez, A.; Alonso, M.; Castro, A.; Perez, C.; Moreno, F. J. First non-ATP competitive glycogen synthase kinase 3β (GSK-3β) inhibitors: Thiadiazolidinones (TDZD) as potential drugs for the treatment of Alzheimer's disease. *J. Med. Chem*. **2002**, *45*, 1292−1299.

(16) Smith, D. G.; Buffet, M.; Fenwick, A. E.; Haigh, D.; Ife, R. J.; Saunders, M.; Slingsby, B. P.; Stacey, R.; Ward, R. W. 3-Anilino-4-arylmaleimides: Potent and selective inhibitors of glycogen synthase kinase-3 (GSK-3). *Bioorg. Med. Chem. Lett*. **2001**, *11*, 635−639.

(17) Coghlan, M. P.; Culbert, A. A.; Cross, D. A. E.; Corcoran, S. L.; Yates, J. W.; Pearce, N. J.; Rausch, O. L.; Murphy, G. J.; Carter, P. S.; Cox, L. R.; Mills, D.; Brown, M. J.; Haigh, D.; Ward, R. W.; Smith, D. G.; Murray, K. J.; Reith, A. D.; Holder, J. C. Selective small molecule inhibitors of glycogen synthase kinase-3 modulate glycogen metabolism and gene transcription. *Chem. Biol*. **2000**, *7* (10), 793−803.

(18) Faul, M. M.; Sullivan, K. A.; Winneroski, L. L. A general approach to the synthesis of bisindolylmaleimides: synthesis of staurosporine aglycone. *Synthesis* **1995**, 1511−1516.

(19) Merz, A.; Karl, A.; Futterer, T.; Stacherdinger, N.; Schneider, O.; Lex, J.; Luboch, E.; Biernat, J. F. Synthesis and reactions of crown ether-bridged stilbenes. *Liebigs Ann. Chem*. **1994**, *12*, 1199−1209.

(20) Faul, M. M.; Winneroski, L. L.; Krumrich, C. A.; Sullivan, K. A.; Gillig, J. R.; Neel, D. A.; Rito, C. J.; Jirousek, M. R. Macrocyclic bisindolylmaleimides: synthesis by inter- and intramolecular alkylation. *J. Org. Chem*. **1998**, *63*, 1961−1973.

(21) Kelly, T. A.; McNeil, D. W.; Rose, J. M.; David, E.; Shih, C.-K.; Grob, P. M. Novel non-nucleoside inhibitors of human immunodeficiency virus type 1 reverse transcriptase. 6. 2-Indol-3-yl- and 2-azaindol-3-yl-dipyridodiazepinones. *J. Med. Chem*. **1997**, *40*, 2430−2433.

(22) Fujita, M.; Oka, H.; Ogura, K. Palladium(0)/LiCl promoted cross-coupling reaction of (4-pyridyl)stannanes and aromatic bromides: easy access to poly-(4-pyridyl)-substituted aromatics. *Tetrahedron Lett*. **1995**, *36*, 5247−5250.

(23) For the less readily available maleimide bromide or maleimide triflate being used in Pd-catalyzed cross-coupling reaction, see the following. (a) Terpin, A.; Winklhofer, C.; Schumann, S.; Steglich, W. Synthesis and cyclization of didemnimide C and its imidazol-1-yl isomer. *Tetrahedorn* **1998**, *54*, 1745−1752. (b) Neel, D. A.; Jirousek, M. R.; McDonald, J. H., III. Synthesis of bisindolylmaleimides using a palladium catalyzed cross-coupling reaction. *Bioorg. Med. Chem. Lett*. **1998**, *8*, 47−50.

(24) Recently, it was reported that condensation of a 7-azaindole Grignard reagent with the less readily available 3,4-dibromo-*N*-methylmaleimide gave bis-7-azaindolylmaleimide. Routier, S.; Ayerbe, N.; Me'rour, J.-Y.; Coudert, G.; Bailly, C.; Pierr'e, A.; Pfeiffer, B.; Caignard, D.-H.; Renard, P. Synthesis and biological evaluation of 7-azaindolocarbazoles. *Tetrahedron* **2002**, *58*, 6621−6630.

(25) Hu, H. Recent discovery and development of selective protein kinase C inhibitors. *Drug Discovery Today* **1996**, *1* (10), 438−447.

(26) Jirousek, M. R.; Gillig, J. R.; Gonzalez, C. M.; Heath, W. F.; McDonald, J. H., III; Neel, D. A.; Rito, C. J.; Singh, U.; Stramm, L. E.; Melikian-Badalian, A.; Baevsky, M.; Ballas, L. M.; Hall, S. E.; Winneroski, L. L.; Faul, M. M. (*S*)-13-[(Dimethylamino)-methyl]-10,11,14,15-tetrahydro-4,9:16,21-dimetheno-1*H*,13*H*-dibenzo[*e*,*k*]pyrrolo[3,4-*h*][1,4,13]oxadiazacyclohexadecene-1,3-(2*H*)-dione (LY333531) and related analogues: Isozyme selective inhibitors of protein kinase Cβ. *J. Med. Chem*. **1996**, *39*, 2664−2671.

(27) Wilkinson, S. E.; Parker, P. J.; Nixon, J. S. Isoenzyme specificity of bisindolylmaleimides, selective inhibitors of protein kinase C. *Biochem. J*. **1993**, *294*, 335−337.

(28) Dekker, L. V.; Parker, P. J. Protein kinase C−a question of specificity. *Trends Biol. Sci*. **1994**, *19*, 73−77.

(29) (a) Leost, M.; Schultz, C.; Link, A.; Yong-Zhong, W.; Biernat, J.; Mandelkow, E.-M.; Bibb, J. A.; Snyder, G. L.; Greengard, P.; Zaharevitz, D. W.; Gussio, R.; Senderowicz, A. M.; Sausville, E. A.; Kunick, C.; Meijer, L. Paullones are potent inhibitors of glycogen synthase kinase-3β and cyclin-dependent kinase 5/p25. *Eur. J. Biochem*. **2000**, *267*, 5983−5944. (b) Leclerc, S.; Garnier, M.; Hoessel, R.; Marko, D.; Bibb, J. A.; Snyder, G. L.; Greengard, P.; Biernat, J.; Wu, Y. Z.; Mandelkow, E. M.; Eisenbrand, G.; Meijer, L. Indirubins inhibit glycogen synthase kinase-3beta and CDK5/p25, two protein kinases involved in abnormal tau phosphorylation in Alzheimer's disease. A property common to most cyclin-dependent kinase inhibitors? *J. Biol. Chem*. **2001**, *276*, 251−260. (c) Mettey, Y.; Gompel, M.; Thomas, V.; Garnier, M.; Leost, M.; Ceballos-Picot, I.; Noble, M.; Endicott, J.; Vierfond, J.-m.; Meijer, L. Aloisines, a new family of CDK/GSK-3 inhibitors. SAR study, crystal structure in complex with CDK2, enzyme selectivity, and cellular effects. *J. Med. Chem*. **2003**, *46*, 222−236.

(30) Hers, I.; Tavare, J. M.; Denton, R. M. The protein kinase C inhibitors bisindolylmaleimide I (GF109203x) and IX (Ro31-8220) are potent inhibitors of glycogen synthase kinase-3 activity. *FEBS Lett*. **1999**, *460*, 433−436.

(31) Kennedy, M. B.; Mcguinness, T.; Greengard, P. Calcium calmodulin dependent protein kinase assay. *J. Neurosci.* **1983**, *3*, 818−831.
(32) The kinetic studies that demonstrated compounds **28** and **29** are ATP competitive inhibitors will be published in a separate manuscript.
(33) Nyfeler, F.; Walter, P. Effect of lithium on glycogen synthesis in hepatocytes from rat liver. *FEBS Lett.* **1979**, *108*, 197−199.
(34) Stambolic, V.; Ruel, L.; Woodgett, J. R. Lithium inhibits glycogen synthase kinase-3 activity and mimics Wingless signaling in intact cells. *Curr. Biol.* **1996**, *6*, 1664−1668.
(35) Klein, P. S.; Melton, D. A. A molecular mechanism for the effect of lithium on development. *Proc. Natl. Acad. Sci. U.S.A.* **1996**, *93*, 8455−8459.
(36) Dajani, R.; Fraser, E.; Roe, S. M.; Young, N.; Good, V.; Dale, T. C.; Pearl, L. H. Crystal structure of glycogen synthase kinase-3 beta. Structural basis for phosphate-primed substrate specificity and autoinhibition. *Cell* **2001**, *105*, 721−732.
(37) Lawrie, A. M.; Noble, M. E.; Tunnah, P.; Brown, N. R.; Johnson, L. N.; Endicott, J. A. Protein kinase inhibition by staurosporine revealed in details of the molecular interaction with CDK2. *Nat. Struct. Biol.* **1997**, *4*, 796−801.
(38) Zhu, X.; Kim, J. L.; Newcomb, J. R.; Rose, P. E.; Stover, D. R.; Toledo, L. M.; Zhao, H.; Morgenstern, K. A. Structure analysis of the lymphocyte-specific kinase Lck in complex with non-selective and Src family selective kinase inhibitors. *Structure (London)* **1999**, *7*, 651−661.
(39) http://pkr.sdsc.edu/html/index.shtml.
(40) Hanks, S.; Quinn, A. M. Protein kinase catalytic domain sequence database: Identification of conserved features of primary structure and classification of family members. *Methods Enzymol.* **1991**, *200*, 38−62.
(41) Davies, S. P.; Reddy, H.; Caivano, M.; Cohen, P. Specificity and mechanism of action of some commonly used protein kinase inhibitors. *Biochem. J.* **2000**, *351*, 95−105.
(42) *SYBYL*, version 6.9; Tripos Inc., 1699 South Hanley Rd, St. Louis, MO, 63144.
(43) Needleman, S. B.; Wunsch, C. D. General method applicable to the search for similarities in the amino acid sequence of two proteins. *J. Mol. Biol.* **1970**, *48*, 443−453.
(44) Chang, G.; Guida, W. C.; Still, W. C. An internal-coordinate Monte Carlo method for searching conformational space. *J. Am. Chem. Soc.* **1989**, *111*, 4379−4386.
(45) *MacroModel*; Schrodinger, 1500 SW First Avenue, Suite 1180, Portland, OR 97201.
(46) *Glide*; Schrodinger, 1500 SW First Avenue, Suite 1180, Portland, OR 97201.
(47) For the full description of GlideScore, see the following. Scoring in Glide. In *First Discovery Technical Notes*; Schrodinger: Portland, OR, 2002; Chapter 5, p 48.
(48) Jorgensen, W. L.; Maxwell, D. S.; Tirado-Rives, J. Development and testing of the OPLS all-atom force field on conformational energetics and properties of organic liquids. *J. Am. Chem. Soc.* **1996**, *118*, 11225−11236.
(49) Still, W. C.; Tempczyk, A.; Hawley, R. C.; Hendrickson, T. Semianalytical treatment of solvation for molecular mechanics and dynamics. *J. Am. Chem. Soc.* **1990**, *112*, 6127−6129.

JM030115O